

Chatter control in the high-speed milling process using μ -synthesis

Niels van Dijk, Nathan van de Wouw, Ed Doppenberg, Han Oosterling and Henk Nijmeijer

Abstract—Chatter is an instability phenomenon in machining processes which limits productivity and results in inferior workpiece quality, noise and rapid tool wear. The increasing demand for productivity in the manufacturing community motivates the development of an active control strategy to shape the chatter stability boundary of manufacturing processes. In this work a control methodology for the high-speed milling process that alters the chatter stability boundary such that the number of chatter-free operating points is increased and a higher productivity can be attained. The methodology developed in this paper is based on a robust control approach using μ -synthesis. Hereto, the most important process parameters (depth of cut and spindle speed) are treated as uncertainties. Effectiveness of the methodology is demonstrated by means of illustrative examples.

I. INTRODUCTION

Chatter is an instability phenomenon in machining processes. The occurrence of (regenerative) chatter results in an inferior workpiece quality due to heavy vibrations of the cutter. Moreover, much noise is produced and the tool wears out rapidly. The occurrence of chatter can be visualised in so-called stability lobes diagrams (SLD). In a SLD the chatter stability boundary between a stable cut (i.e. without chatter) and an unstable cut (i.e. with chatter) is visualised in terms of spindle speed and depth of cut.

In the present day manufacturing industry, an increasing demand for high-precision products at a high productivity level is posed. This motivates the desire for the design of dedicated control strategies, which are able to actively alter the chatter stability boundary. Hence, this paper presents a control methodology for the high-speed milling process that alters the chatter stability boundary such that the number of chatter-free operating points is increased and a higher productivity can be attained.

Basically three methods exist in literature to control chatter. The first method to avoid chatter is to adjust process parameters (i.e. spindle speed, feed per tooth or chip load) such that a stable working point is chosen [1], [2]. Although chatter can be eliminated by adaptation of process parameters, the methodology does not enlarge the domain of stable operation points towards those of higher productivity.

A second method is to disturb the regenerative effect by continuous spindle speed modulation [3], [4]. Although the stability boundary is altered by spindle speed modulation

[5], the method cannot be used in the case of high-speed milling since the modulation speed is limited by the inertia and actuation power of the spindle. The third method is to passively or actively alter the machine dynamics to alter the chatter boundary. There are passive chatter suppression techniques that use dampers [6] or vibration absorbers [7]. Passive dampers are relatively cheap and easy to implement and never destabilise the system. However, the practically achievable amount of damping is rather limited. Moreover, vibration absorbers require accurate tuning of their natural frequencies and, consequently, lack robustness to changing machining conditions. Active chatter control in milling has mainly been focused on active damping of machine dynamics [8], [9] or workpiece [10]. Damping the machine or workpiece dynamics, either passively or actively, results in a uniform increase of the stability boundary for all spindle speeds. To enable more dedicated shaping of the stability boundary (e.g. lifting the SLD locally around a specific spindle speed), the regenerative effect should be taken into account during chatter controller design. In [11], an optimal state feedback-observer controller with integral control in the case of turning was designed. Recently, Chen and Knospe [12] developed three different chatter control strategies in the case of turning: speed-independent control, speed-specified control and speed-interval control. Except for the work in [9], all research on active chatter control is limited to low spindle speeds (i.e. below 5000 rpm).

In this paper, an active chatter controller methodology for the high-speed milling process is presented, which can guarantee chatter-free cutting operations in an a priori defined range of process parameters such as spindle speed and depth of cut. Current chatter control strategies for the milling process cannot provide such a strong condition. In general, the existing techniques require a posteriori calculation of the set of stable working points. The methodology developed in this paper is based on a robust control approach using μ -synthesis. Hereto, the most important process parameters (depth of cut and spindle speed) are treated as uncertainties. The proposed methodology will allow the machinist to define a desired working range (in spindle speed and depth of cut) and lift the SLD locally in a dedicated fashion. Moreover, in practice the maximum actuator force is limited. Hence, robust stabilisation of high-speed milling operations while minimising the control effort is considered. Effectiveness of the proposed control methodology is shown by means of an illustrative example.

II. THE MILLING PROCESS

This section presents a comprehensive model of the milling process which describes regenerative chatter. Stability prop-

This work is supported by the Dutch Ministry of Economic affairs within the framework of Innovation Oriented Research Programmes (IOP) Precision Technology.

Niels van Dijk, Nathan van de Wouw and Henk Nijmeijer are with the Department of Mechanical Engineering, Eindhoven University of Technology, P.O. Box 513, 5600 MB Eindhoven, The Netherlands, N.J.M.v.Dijk@tue.nl

E.J.J. Doppenberg and J.A.J. Oosterling are with TNO Science and Industry, P.O. Box 6235, 5600 HE Eindhoven, The Netherlands.

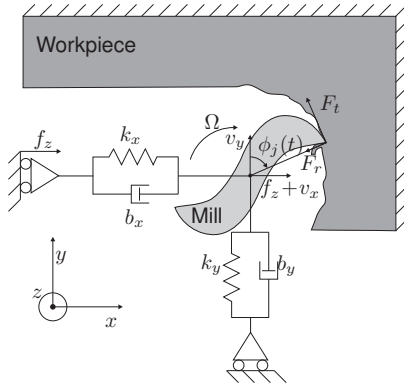


Fig. 1: Schematic representation of the milling process.

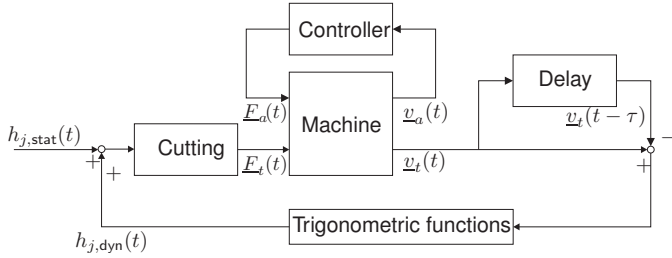


Fig. 2: Block diagram of the milling process.

erties of the model will be discussed. Moreover, for the purpose of controller design some model simplifications are necessary which will be treated subsequently.

A. A comprehensive milling model

In Figure 1, a schematic representation of the milling process is given. A block diagram of the milling process, with controller, is given in Figure 2. As can be seen from the block diagram, the milling process is a closed-loop position-driven process. The setpoint of the milling process is the predefined motion of the tool with respect to the workpiece, given in terms of the static chip thickness $h_{j,stat}(t) = f_z \sin \phi_j(t)$, where f_z is the feed per tooth and $\phi_j(t)$ the rotation angle of the j -th tooth of the tool with respect to the y (normal) axis (see Figure 1). However, the total chip thickness $h_j(t)$ also depends on the interaction between the cutter and the workpiece. This leads to cutter vibrations resulting in a dynamic displacement $\underline{v}_t(t)$ of the tool which is superimposed on the predefined tool motion. This results in a wavy surface on the workpiece. The next tooth encounters the wavy surface, left behind by the previous tooth, and generates its own waviness. This is called the regenerative effect and results in the block **Delay** in Figure 2 see [13]. The difference between the current and previous wavy surface is denoted as the dynamic chip thickness $h_{j,dyn}(t) = \underline{v}_t(t) - \underline{v}_t(t - \tau)$ with τ the delay. Hence, the total chip thickness of tooth j , $h_j(t)$, is the sum of the static and dynamic chip thickness, $h_j(t) = h_{j,stat}(t) + h_{j,dyn}(t)$.

The cutting force model (indicated by the **Cutting** block in Figure 2) relates the total chip thickness to the forces acting at the tool tip of the machine spindle. The forces in tangential and radial direction for a single tooth j are described by the

following exponential cutting force model:

$$\begin{aligned} F_{t_j}(t) &= g_j(\phi_j(t)) K_t a_p h_j(t)^{x_F}, \\ F_{r_j}(t) &= g_j(\phi_j(t)) K_r a_p h_j(t)^{x_F}, \end{aligned} \quad (1)$$

where $0 < x_F \leq 1$ and $K_t, K_r > 0$ are cutting parameters which depend on the workpiece material, and a_p is the axial depth of cut. The function $g_j(\phi_j(t))$ describes whether a tooth is in or out of cut:

$$g_j(\phi_j(t)) = \begin{cases} 1, & \phi_s \leq \phi_j(t) \leq \phi_e \wedge h_j(t) > 0, \\ 0, & \text{else,} \end{cases} \quad (2)$$

where ϕ_s and ϕ_e are the entry and exit angle of the cut, respectively. Via trigonometric functions, the cutting force can easily be converted to x (feed)- and y (normal)-direction. Hence, cutting forces in x - and y -direction can be obtained by summing over all z teeth:

$$\begin{aligned} \underline{F}(t) &= a_p \sum_{j=0}^{z-1} g_j(\phi_j(t)) \left(\left(h_{j,stat}(t) \right. \right. \\ &\quad \left. \left. + [\sin \phi_j(t) \cos \phi_j(t)] (\underline{v}_t(t) - \underline{v}_t(t - \tau)) \right)^{x_F} \right. \\ &\quad \left. \mathbf{S}(t) \begin{bmatrix} K_t \\ K_r \end{bmatrix} \right), \end{aligned} \quad (3)$$

where

$$\mathbf{S}(t) = \begin{bmatrix} -\cos \phi_j(t) & -\sin \phi_j(t) \\ \sin \phi_j(t) & -\cos \phi_j(t) \end{bmatrix}.$$

The cutting force interacts with the spindle and tool dynamics (block **Machine**) in Figure 2. The machine dynamics are modelled via a linear multi-input-multi-output (MIMO) state-space model,

$$\begin{aligned} \dot{\underline{q}}(t) &= \mathbf{A}\underline{q}(t) + \mathbf{B}_t \underline{F}_t(t) + \mathbf{B}_a \underline{F}_a(t), \\ \underline{v}_t(t) &= \mathbf{C}_t \underline{q}(t), \quad \underline{v}_a(t) = \mathbf{C}_a \underline{q}(t), \end{aligned} \quad (4)$$

where $\underline{q}(t)$ is the state (the order of this model primarily depends on the order of the spindle-tool dynamics model) and cutting forces $\underline{F}_t(t) = [F_{t,x}(t) \ F_{t,y}(t)]^T$, where $F_{t,x}(t)$ and $F_{t,y}(t)$ are the cutting forces in x - and y -direction, respectively. The control forces are given by $\underline{F}_a(t) = [F_{a,x}(t) \ F_{a,y}(t)]^T$, where $F_{a,x}(t)$ and $F_{a,y}(t)$ are the control forces acting in x - and y -direction, respectively. Moreover, $\underline{v}_t(t)$ and $\underline{v}_a(t)$ are the displacements of the cutter and the measured displacements available for feedback, respectively.

Substitution of (3) into (4) yields the nonlinear, non-autonomous delay differential equations (DDE) describing the milling process:

$$\begin{aligned} \dot{\underline{q}}(t) &= \mathbf{A}\underline{q}(t) + \mathbf{B}_t a_p \sum_{j=0}^{z-1} g_j(\phi_j(t)) \left(\left(h_{j,stat}(t) + \right. \right. \\ &\quad \left. \left. [\sin \phi_j(t) \cos \phi_j(t)] \mathbf{C}_t (\underline{q}(t) - \underline{q}(t - \tau)) \right)^{x_F} \right. \\ &\quad \left. \mathbf{S}(t) \begin{bmatrix} K_t \\ K_r \end{bmatrix} \right) + \mathbf{B}_a \underline{F}_a(t), \\ \underline{v}_a(t) &= \mathbf{C}_a \underline{q}(t). \end{aligned} \quad (5)$$

B. Stability of the milling process

In the milling process the static chip thickness is periodic with period time $\tau = \frac{60}{zn}$. Here n is the spindle speed in revolutions per minute (rpm). In general, the milling model (5) has a periodic solution $\underline{q}^*(t)$ with period time τ [14]. When no chatter occurs, the periodic solution is (at least locally) asymptotically stable and when chatter occurs it is unstable. Therefore, the chatter stability boundary can be found by studying the (local) stability of the periodic solution. To this end, the milling model is linearised about the periodic solution $\underline{q}^*(t)$ for zero control input (i.e. $\underline{F}_a(t) = \underline{0}$) which yields the following linearised dynamics in terms of perturbations $\tilde{q}(t)$ ($\underline{q}(t) = \underline{q}^*(t) + \tilde{q}(t)$):

$$\begin{aligned} \dot{\tilde{q}}(t) &= \mathbf{A}\tilde{q}(t) + a_p \mathbf{B}_t \sum_{j=0}^{z-1} \mathbf{H}_j(t) \mathbf{C}_t (\tilde{q}(t) - \tilde{q}(t - \tau)) \\ &+ \mathbf{B}_a \underline{F}_a(t), \tilde{\underline{v}}_a(t) = \mathbf{C}_a \tilde{q}(t), \end{aligned} \quad (6)$$

where

$$\mathbf{H}_j(t) = g_j x_F (f_z \sin \phi_j)^{x_F-1} \mathbf{S}(t) \begin{bmatrix} K_t \\ K_r \end{bmatrix} \begin{bmatrix} \sin \phi_j & \cos \phi_j \end{bmatrix}. \quad (7)$$

As can be seen from (6) the linearised model is a *nonautonomous* DDE. The focus in this work lies on full immersion cuts, where the full width of the cutter is used for cutting. As described in [15], for full immersion cuts it is sufficient to average the dynamic cutting forces $\sum_{j=0}^{z-1} \mathbf{H}_j(t)$ over the tool path such that the milling model becomes an *autonomous* (time-invariant) DDE model. Since the cutter is only cutting when $\phi_s \leq \phi \leq \phi_e$ the averaged cutting forces are given by

$$\bar{\mathbf{H}} = \frac{z}{2\pi} \int_{\phi_s}^{\phi_e} \sum_{j=0}^{z-1} \mathbf{H}_j(\phi) d\phi. \quad (8)$$

The characteristic equation of the linear DDE (6), with $\mathbf{H}_j(t) = \bar{\mathbf{H}}$ and $\bar{\mathbf{H}}$ given in (8), is then given as

$$\det(\mathbf{I} - a_p \mathbf{G}_{tt}(i\omega) \bar{\mathbf{H}}(1 - e^{-i\omega\tau})) = 0, \quad (9)$$

where $\mathbf{G}_{tt}(i\omega) = \mathbf{C}_t(i\omega \mathbf{I} - \mathbf{A})^{-1} \mathbf{B}_t$ represents the frequency response function (FRF) from cutting forces at the tooltip to tooltip displacements. The chatter stability boundary can be obtained by solving (9) for depth-of-cut a_p and delay τ as e.g. discussed in [15].

C. Model simplification for control

The model (6), with $\mathbf{H}_j(t) = \bar{\mathbf{H}}$ and $\bar{\mathbf{H}}$ given in (8), can readily be employed for stability analysis (i.e. determination of the SLD). However, the presence of time-delay complicates the development of robust control synthesis techniques. Here, we apply a finite-dimensional approximation using a Padé approximation (see also [11], [12]). Hereto, the delayed tool vibrations $\tilde{\underline{v}}_t(t - \tau) = \mathbf{C}_t \tilde{q}(t - \tau)$ is approximated by Padé approximation denoted by $\tilde{v}_p(t)$, such that $\tilde{\underline{v}}_t(t - \tau) = \mathbf{C}_t \tilde{q}(t - \tau) \approx \tilde{\underline{v}}_p(t)$. The milling model in (6) with cutting force averaging, defined in (8), and Padé approximation is

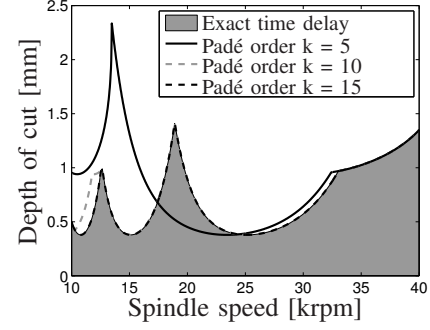


Fig. 3: Stability lobes diagram for the milling process with Padé approximation of order k and the milling model with exact time delay.

TABLE I: Milling model parameters.

Parameter	Value	Parameter	Value
$m_{t,x} = m_{t,y}$	0.015 kg	K_t	462 [N/mm ^(1+x_F)]
$m_{a,x} = m_{a,y}$	0.14 kg	K_r	38.6 [N/mm ^(1+x_F)]
$\omega_{t,x} = \omega_{t,y}$	2350 Hz	x_F	0.744 [-]
$\omega_{a,x} = \omega_{a,y}$	1400 Hz	ϕ_s	0 [rad]
$\zeta_{t,x} = \zeta_{t,y}$	0.05 [-]	ϕ_e	π [rad]
$\zeta_{a,x} = \zeta_{a,y}$	0.12 [-]	f_z	0.2 mm/tooth
z	4 [-]		

given as,

$$\begin{aligned} \begin{bmatrix} \dot{\tilde{q}}(t) \\ \tilde{\underline{q}}_p(t) \end{bmatrix} &= \begin{bmatrix} \mathbf{A} + a_p \mathbf{B}_t \bar{\mathbf{H}} (\mathbf{C}_t - \mathbf{D}_p \mathbf{C}_t) & -a_p \mathbf{B}_t \bar{\mathbf{H}} \mathbf{C}_t \\ \mathbf{B}_p \mathbf{C}_t & \mathbf{A}_p \end{bmatrix} \begin{bmatrix} \tilde{q}(t) \\ \tilde{\underline{q}}_p(t) \end{bmatrix} \\ &+ \begin{bmatrix} \mathbf{B}_a \\ \mathbf{0} \end{bmatrix} \underline{F}_a(t), \tilde{\underline{v}}_a(t) = \mathbf{C}_a \tilde{q}(t), \end{aligned} \quad (10)$$

where $\mathbf{A}_p, \mathbf{B}_p, \mathbf{C}_p$ and \mathbf{D}_p denote matrices of the state-space description of the Padé approximation. The size of these matrices depends on the chosen order k for the Padé approximation. The order of the Padé approximation will be based on a desired level of accuracy regarding the predicted chatter stability boundary using the model with Padé approximation.

In Figure 3 the chatter stability boundary is given for the model with time-delay obtained by solving (9), and for different orders k of Padé approximation. Hereto, the machine spindle-toolholder-tool dynamics is modelled by two decoupled subsystems consisting of two mass-spring-damper systems, with masses $m_{a,j}, m_{t,j}$ $j = x, y$ eigenfrequencies $\omega_{a,j}, \omega_{t,j}$ $j = x, y$ and damping ratios $\zeta_{a,j}, \zeta_{t,j}$ $j = x, y$. This in order to capture the inherent dynamics between the actuator/sensor system (denoted by subscript a) and the cutting tool (denoted by subscript t). The parameters of the machine spindle model and cutting force coefficients are listed in Table I. From Figure 3 it can be observed that, for increasing order k of the Padé approximation, the error between the stability lobes determined using the exact delay term and the approximated delay term becomes smaller. Moreover, since the delay is inversely proportional to the spindle speed, the approximation becomes more accurate as the spindle speed increases. Here we focus on high-spindle speeds (i.e. above 15 krpm). Hence, throughout this paper the order of the Padé approximation is chosen equal to $k = 10$.

III. ROBUST CONTROLLER DESIGN

This section describes the controller design for an active chatter control methodology that will alter the chatter stability boundary, such that stable operating points, reflecting higher productivity, can be attained.

A. Control objective

As outlined in the introduction, we aim to design a controller such that the milling process is stabilised for a pre-defined area of working points (in terms of depth-of-cut a_p and spindle speed n) for bounded control effort. This control problem can be cast into the μ -synthesis framework. The set of milling operations to be stabilised will be expressed as uncertainties in depth of cut a_p and spindle speed n .

B. Nominal model

Given the milling process, modelled as in (10), as discussed in the previous section, we propose to design a linear dynamic controller with transfer function

$$\mathbf{K}(s) = \begin{bmatrix} K_{xx}(s) & K_{xy}(s) \\ K_{yx}(s) & K_{yy}(s) \end{bmatrix}, \quad (11)$$

$s \in \mathbb{C}$, from measured perturbation displacements $\tilde{\underline{u}}_a$ to actuator forces \underline{F}_a to effectively adapt the spindle dynamics. However, in contrast to most active chatter control methods discussed in the introduction, in this work we do not only consider the spindle dynamics during the control design, but also take the interaction between the spindle dynamics and the cutting forces into account. Equation (10) gives the nominal plant model used during μ -synthesis.

C. Uncertainty modelling

This section describes the modelling of the uncertainties in the process parameters, which can be considered as a key step in achieving the control objective defined above: robust stability (i.e. chatter avoidance) in a range of process parameters.

First, the uncertainty in depth of cut a_p is considered which is modelled as a parametric uncertainty $a_{p,u}$. An important (practical) aspect is that robust control design should provide stability for small as well as (relatively) large values of the depth of cut. Hereto, the uncertain depth of cut is modelled such that it specifies a range from zero up to a maximum value, i.e. $a_{p,u} \in [0, \bar{a}_p]$. Let us define a real scalar uncertainty set $\Delta_{a_p} = \{\delta_{a_p} \in \mathbb{R} \mid \|\delta_{a_p}\| \leq 1\}$. The uncertainty for the depth of cut is then defined by

$$a_{p,u} \in \frac{1}{2}\bar{a}_p(1 + \Delta_{a_p}), \quad (12)$$

where \bar{a}_p is the maximal depth of cut for which stable cutting is desired.

The uncertainty in the time-delay τ (and thus spindle speed) is formulated as considered by Chen and Knospe [12]. Hereto, note that for arbitrary frequency ω , the value set of $e^{-i\omega\tau}$ for all $\tau \in [\underline{\tau}, \bar{\tau}]$ can be represented in the complex plane as a circular arc extending along the unit circle. Then, this time-delay interval can be approximated by choosing any stable transfer functions $G_d(s)$ and $W_d(s)$ such that $G_d(s) + W_d(s)\Delta_d$, with $\Delta_d \in \mathbb{C}$ and $|\Delta_d| \leq 1$,

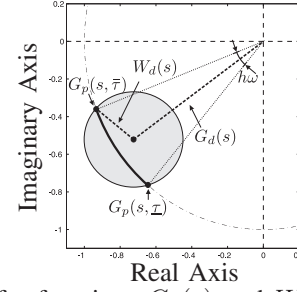


Fig. 4: Transfer functions $G_d(s)$ and $W_d(s)$ to cover of a range of Padé approximations $G_p(s, \tau)$ of $e^{-s\tau}$ of interval time-delay $\tau \in [\underline{\tau}, \bar{\tau}]$ (based on [12]).

covers the interval delay element, as shown in Figure 4. In order to reduce conservatism, Chen and Knospe propose to choose $G_d(s)$ and $W_d(s)$ such that at each frequency: 1) the arc length covered by the disk is nearly that of the delay element and 2) the area of the disk lying outside the unit circle is minimised. Then, stable filter $G_d(s)$ is defined as follows [12]

$$G_d(s) = \left(\frac{G_{pn}(0)}{G_{pd}(s)} \right)^2, \quad (13)$$

where $G_p(s) = G_{pn}(s)/G_{pd}(s)$ and a lower bound for the magnitude of the filter $W_d(s)$ can be calculated as:

$$\sqrt{1 + |G_d(j\omega)|^2 - 2|G_d(i\omega)| \cos \frac{h\omega}{2}} \leq |W_d(i\omega)|. \quad (14)$$

The filter $W_d(s)$ is then obtained by fitting the magnitude with a stable minimum-phase transfer function.

D. Performance requirement

In essence, the chatter control problem at hand is a robust stabilisation problem. This robust stability requirement has to be achieved with limited control effort, since actuator forces can not become infinitely large. Therefore, the control input to the system ($\underline{F}_a(t)$) will be limited during μ -synthesis.

Limiting the control input ($\underline{F}_a(t)$) is done by applying a performance requirement to the control problem, in terms of an upper bound on the control sensitivity $\mathbf{KS}(s) = \mathbf{K}(s)(\mathbf{I} - \mathbf{K}(s)\mathbf{P}(s))^{-1}$, where $\mathbf{P}(s)$ gives the transfer function representation of the nominal plant given by (10). Here, the control sensitivity is defined as the transfer function from a input signal $r(t)$ (which can e.g. be interpreted as measurement noise entering the feedback loop) to the control input $\underline{F}_a(t)$. The bound on the control sensitivity is enforced by defining a weighting function $\mathbf{W}_{KS}(s) = W_{KS}(s)\mathbf{I}$, where $W_{KS}(s)$ is written as:

$$W_{KS}(s) = K_p \frac{\frac{1}{2\pi f_r} s + 1}{\frac{1}{2\pi f_p} s + 1}. \quad (15)$$

The structure of $W_{KS}(s)$ is chosen such that, for frequencies larger than a roll-off frequency f_r , the inputs to the controller are attenuated in order to reduce the (undesired) influence of high-frequent measurement noise on the control action. Moreover, K_p denotes the static control gain and a pole, at frequency f_p (such that $f_p > f_r$), is added to obtain a proper weighting function, necessary for implementation.

IV. RESULTS

In this section, the actual controller synthesis is addressed. In order to demonstrate the feasibility of the μ -synthesis approach proposed in the previous section, control design is performed for an illustrative example.

Hereto, consider the parameters of the milling process as given in Table I. The spindle dynamics is modelled, as before, by two decoupled subsystems consisting of a two mass-spring-damper model in order to capture the inherent compliance between the actuator/sensor system (with mass $m_{a,j}$ $j = x, y$) and the cutting tool (with mass $m_{t,j}$ $j = x, y$).

Controllers are sought that stabilise milling operations for a single spindle speed as well as for a spindle speed interval, for a range of depth-of-cut a_p which should be as large as possible for the given performance requirement (in this case the bound on the control sensitivity $\mathbf{KS}(s)$). Hereto, μ -synthesis is employed within a bi-section scheme.

From the uncertainty models, presented in the previous section, it can be concluded that we are dealing with a so-called mixed μ -synthesis problem, i.e. both complex and real uncertainty sets are present. Although, mixed μ -synthesis can be employed via D,G-K-iteration [16], it will in general result in high-order controllers due to high-order fits required for the G-scales. As the general plant in this work is of relatively high order (since a relatively high-order Padé approximation is needed to accurately approximate the time delay), the uncertainty in depth-of-cut is considered as a complex uncertainty and controller design is employed using D-K-iteration. We accept the additional conservatism introduced by considering only complex uncertainties during the controller design over a controller of even higher order.

The performance requirement, presented in the previous section, is used to limit the control forces. Hereto, the upper bound on the control sensitivity gain is set to $K_p = 1 \cdot 10^{-6}$ mm/N. Moreover, $f_r = 7500$ Hz and $f_p = 1e5$ Hz, where the roll of frequency is set to approximately three times the largest eigenfrequency of the machine spindle and the extra pole is chosen arbitrarily.

The results are presented where controllers $\mathbf{K}(s)$ are designed for a single spindle speed $n = 27000$ and a spindle speed interval $n \in [34000, 36000]$ rpm. A 10-th order Padé approximation is used to construct $\mathbf{G}_p(s)$ (and $\mathbf{G}_d(s)$) and a 6-th order weighting function $W_d(s)$ is used for the case with spindle speed uncertainty. Controller synthesis using D-K-iteration yields a 38-th order controller for a maximal depth of cut of $\bar{a}_p = 2.75$ mm ($\mu = 0.995$) for $n = 27000$ rpm and a 62-th order controller for a maximal depth of cut of $\bar{a}_p = 2.25$ mm ($\mu = 0.98$) for $n \in [34000, 36000]$ rpm. The higher order of the controller with spindle speed uncertainty, compared to the fixed spindle speed case, is mainly due to the delay uncertainty modelling. To reduce the controller order, (closed-loop) model reduction techniques can be applied, see e.g. [17]. We leave this topic for future work.

Frequency response functions (FRF) of the obtained controllers together with the inverse of the frequency bound imposed on the control sensitivity (i.e. $W_{KS}^{-1}(s)$) are given in Figure 5. It can be seen that the resulting controllers

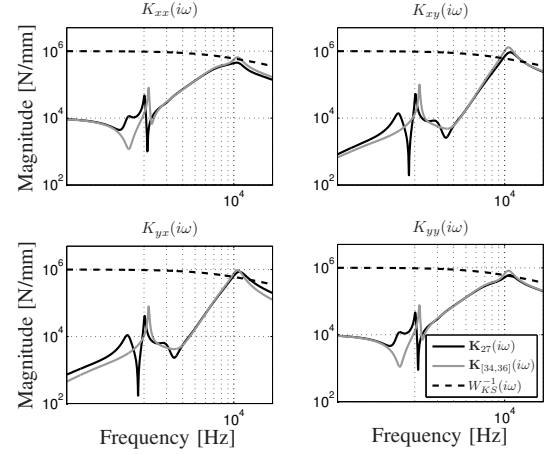


Fig. 5: Magnitude of FRF of the controllers obtained by D-K-iteration for fixed spindle speeds $n = 27000$ (black) and $n \in [34000, 36000]$ rpm (grey).

exhibit highly dynamical characteristics indicated by the inverse notches in the FRF. However, for the spindle speed interval case, the (inverse) notch-like characteristics exhibit more damping. Although the magnitude of the controllers do not exactly fulfill the imposed bound (since the bound is imposed on the control sensitivity $\mathbf{KS}(s)$), it can be seen that the magnitude is bounded. In Figure 6(a) the SLD for the case with and without control can be found. The SLDs are determined using the original milling model (6) (i.e. with time delay), with $\mathbf{H}_j(t) = \bar{\mathbf{H}}$ and $\bar{\mathbf{H}}$ given in (8), as outlined in Section II-B. Figure 6(a) clearly illustrates the power of the proposed approach, as the SLD is shaped to guarantee robust stability for the desired range of depth of cut and spindle speed (while avoiding chatter and satisfying a specified bound on the control gain). Due to conservatism of the delay approximation, for the case with spindle speed uncertainty, stability is guaranteed for an area somewhat larger than the domain to be stabilised. For the fixed spindle speed case, stability is increased at the desired spindle speeds, while it decreases significantly at the remaining spindle speeds. This can be explained by examining the controlled machine dynamics.

The FRF of the closed-loop tool-tip spindle dynamics $\mathbf{G}_{tt,c}(s)$ (i.e. the FRF from $\hat{\underline{F}}_t(t)$ to $\hat{\underline{v}}_t(t)$) is given, together with the original (uncontrolled) spindle dynamics, in Figure 6(b). While the original (uncontrolled) spindle dynamics only has x - and y -components, the controlled machine dynamics also has off-diagonal components. This results from the fact that the nominal plant contains a coupling between x - and y -direction terms introduced by the cutting force model (resulting in a full matrix $\bar{\mathbf{H}}$ and consequently in a full 2×2 controller $\mathbf{K}(s)$). It can be seen that the fixed spindle speed controller tailors the spindle dynamics such that a dominant weakly-damped resonance is created. The frequency at which this dominant resonance is situated is $f = 1800$ Hz which corresponds to the tooth excitation frequency $f_{tpe} = \frac{nz}{60}$ at this spindle speed. Hence, it can be concluded that, in order to create a stability lobe at a certain spindle speed, the natural frequency of the spindle dynamics should be set equal to the corresponding tooth passing excitation frequency.

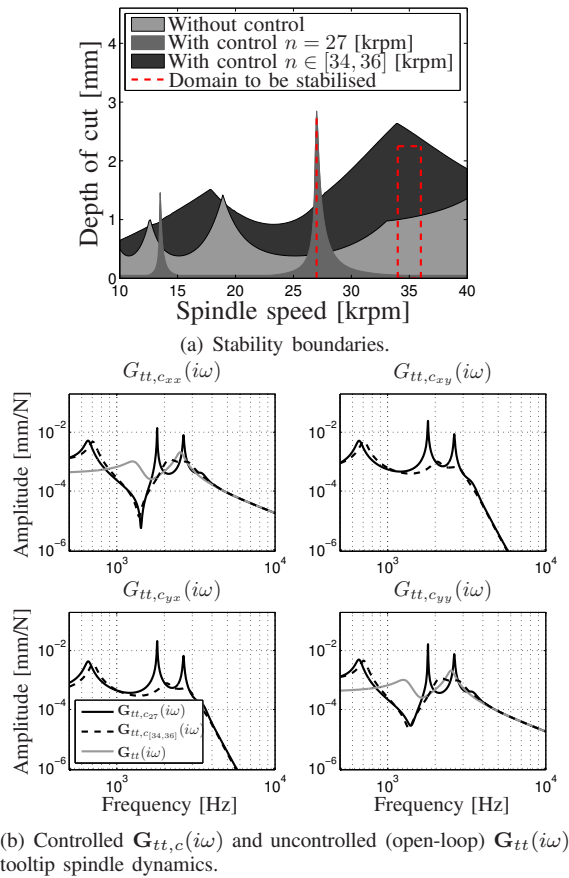


Fig. 6: Stability boundaries and tooltip spindle dynamics for controllers designed for fixed spindle speed, $n = 27000$ (black) and $n \in [34000, 36000]$ rpm (grey).

Robustness for a range of spindle speeds (dashed line in Figure 6(b)) results in better damped modes as compared to the fixed spindle speed case. The fact that a closed-loop spindle resonance is situated at a tooth-passing excitation frequency can be explained as follows. In the milling process the highest depth of cut can be obtained when the dynamic chip thickness $h_{j,dyn}(t) = \underline{v}_t(t) - \underline{v}_t(t - \tau)$ is equal to zero. This relation can be transformed to the frequency domain as follows

$$H_{j,dyn}(i\omega) = (1 - e^{-i\omega\tau})V_t(i\omega) = : Q(i\omega)V_t(i\omega). \quad (16)$$

Hence, the difference between the present and previous cut is actually a filter, denoted by $Q(i\omega)$, with zeros at $l\omega\tau = l\omega\frac{1}{f_{tpe}}$, $l = 0, 1, \dots$. Moreover, for the milling process, the dominant (chatter) frequency of the perturbation vibrations lies in general close to the eigenfrequency of the spindle dynamics [14]. Then, by designing the controller such that the closed-loop resonance of the spindle dynamics is close to a tooth-passing frequency and due to the filter properties of the $Q(i\omega)$, this results in the dynamic chip thickness to be zero at the desired spindle speed, resulting in a large depth of cut.

V. CONCLUSIONS

This paper proposes a control methodology in which the problem of actively controlling regenerative chatter in

the high-speed milling process is addressed. Herein, the requirement for a priori stability for a predefined range of process parameters is cast into a robust stability requirement. The control problem is solved via μ -synthesis using D-K-iteration. A comprehensive milling model is presented which, due to the presence of a time-delay, complicates the development of robust control synthesis techniques. Hereto, a finite-dimensional approximation of the time delay is applied during controller synthesis. The set of milling operations to be stabilised are expressed as uncertainties in the process parameters depth of cut and spindle speed. Moreover, a performance requirement is imposed on the control sensitivity in order to limit the actuator forces. Results, for illustrative examples, show the power of the proposed control methodology. The chatter stability boundary is locally shaped to stabilise the desired range of working points.

REFERENCES

- [1] S. Smith and T. Delio, "Sensor-based chatter detection and avoidance by spindle speed," *Journal of dynamic systems, measurement and control*, vol. 114, no. 3, pp. 486–492, 1992.
- [2] N. van Dijk, E. Doppenberg, R. Faassen, N. van de Wouw, J. Oosterling, and H. Nijmeijer, "Automatic in-process chatter avoidance in the high-speed milling process," *Journal of dynamic systems, measurement and control*, Accepted 2010.
- [3] A. Yilmaz, E. AL-Regib, and J. Ni, "Machine tool chatter suppression by multi-level random spindle speed variation," *Journal of manufacturing science and engineering*, vol. 124, no. 2, pp. 208–216, 2002.
- [4] E. Soliman and F. Ismail, "Chatter suppression by adaptive speed modulation," *International Journal of Machine Tools and Manufacture*, vol. 37, no. 3, pp. 355–369, Mar. 1997.
- [5] T. Insperger and G. Stépán, "Stability analysis of turning with periodic spindle speed modulation via semi-discretisation," *Journal of vibration and control*, vol. 10, pp. 1835–1855, 2004.
- [6] K. Liu and K. Rouch, "Optimal passive vibration control of cutting process stability in milling," *Journal of materials processing technology*, vol. 28, no. 1-2, pp. 285–294, 1991.
- [7] Y. Tarn, J. Kao, and E. Lee, "Chatter suppression in turning operations with a tuned vibration absorber," *Journal of materials processing technology*, vol. 105, no. 1, pp. 55–60, 2000.
- [8] J. Dohner, J. Lauffer, T. Hinnerichs, N. Shankar, M. Regelbrugge, C. Kwan, R. Xu, B. Winterbauer, and K. Bridger, "Mitigation of chatter instabilities in milling by active structural control," *Journal of sound and vibration*, vol. 269, no. 1-2, pp. 197–211, 2004.
- [9] S. Kern, C. Ehmann, R. Nordmann, M. Roth, A. Schiffler, and E. Abele, "Active damping of chatter vibrations with an active magnetic bearing in a motor spindle using μ -synthesis and an adaptive filter," in *The 8th Int. Conf. on Motion and Vibration Control*, 2006.
- [10] Y. Zhang and N. Sims, "Milling workpiece chatter avoidance using piezoelectric active damping: A feasibility study," *Smart materials and structures*, vol. 14, no. 6, pp. N65–N70, 2005.
- [11] M. Shiraishi, K. Yamanaka, and H. Fujita, "Optimal control of chatter in turning," *International journal of machine tools and manufacture*, vol. 31, no. 1, pp. 31–43, 1991.
- [12] M. Chen and C. Knospe, "Control approaches to the suppression of machining chatter using active magnetic bearings," *IEEE Transactions on control systems technology*, vol. 15, no. 2, pp. 220–232, 2007.
- [13] H. Merritt, "Theory of self-excited machine-tool chatter," *Journal of engineering for industry, Transaction of the ASME*, vol. 87, no. 4, pp. 447–454, 1965.
- [14] T. Insperger, G. Stépán, P. V. Bayly, and B. P. Mann, "Multiple chatter frequencies in milling processes," *Journal of sound and vibration*, vol. 262, no. 2, pp. 333–345, Apr. 2003.
- [15] Y. Altintas, *Manufacturing automation*. Cambridge, UK: Cambridge University Press, 2000.
- [16] P. Young, "Robustness with parametric and dynamic uncertainty," Ph.D. dissertation, California institute of technology, 1993.
- [17] P. Wortelboer, "Frequency-weighted balanced reduction of closed-loop mechanical servo-systems," Ph.D. dissertation, Delft University of Technology, 1994.